Available online at www.sciencedirect.com
SCIENCE DIRECT®

Journal of the European Ceramic Society 24 (2004) 139–146

www.elsevier.com/locate/jeurceramsoc

Effects of dopants and hydrogen on the electrical conductivity of ZnO

Zhen Zhou[a,*], K. Kato[a], T. Komaki[a], M. Yoshino[a], H. Yukawa[a], M. Morinaga[a], K. Morita[b]

[a]*Department of Materials Science and Engineering, Graduate School of Engineering, Nagoya University, Furo-cho, Chikusa-ku, Nagoya 464-8603, Japan*
[b]*Department of Nuclear Engineering, Graduate School of Engineering, Nagoya University, Furo-cho, Chikusa-ku, Nagoya 464-8603, Japan*

Received 19 December 2002; received in revised form 4 April 2003; accepted 27 April 2003

Abstract

The effects of dopants on the electrical conductivity of ZnO were investigated through the ac impedance spectroscopy. The doping of Al increased the electrical conductivity of ZnO greatly, whereas the doping of Li decreased it both in the grain and in the grain boundary. The doping of the 3d transition metals (Co, Mn, and Cu) made the grain boundary more resistive, but the doping effect on the electrical conductivity inside the grain was varied depending on the doping elements. The doping of Co had no significant effects on the electrical conductivity of the grain, and the doping of Mn made the grain a little more resistive. The doping of Cu made the grain much more resistive. In addition, hydrogen was introduced into ZnO by the ion implantation method. The electrical conductivity in the hydrogen-implanted ZnO layer increased by four orders of magnitude. The mechanisms for the doping effects were discussed in this investigation.

Keywords: Electrical conductivity; Impedance; Impurities; Sintering; ZnO

1. Introduction

Wurtzitic ZnO is a wide-bandgap semiconductor (3.437 eV at 2 K), widely used in piezoelectric transducers, varistor, gas sensor, catalyst, and transparent conducting films.[1–5] In the use for electronic components such as piezoelectric transducers and varistor, the effects of dopants are very important. Typical ZnO based varistor is a very complex chemical system containing several dopants, such as Bi, Pr, Mn, Co, Cu, Sb, V, Cr an Al.[2,6–10] The electrical properties of ZnO are related closely to the composition and the microstructure. So it is important to understand the effects of the individual additives in a fundamental manner. There were some reports on the above doping elements in the ZnO varistor or thin film, but the effects of some doping elements on the grain and grain boundary of ZnO still remain unclear, because the doping effects have been studied in quite different systems under different experimental conditions, and the effect of individual dopant might be complicated by other dopants in ZnO with multi-components. Therefore, it is necessary to investigate the various dopants independently in a systemic way to understand the role of each dopant in the electrical properties of ZnO. Recently, Han et al have studied the effects of Al and Mn doping on the electrical conductivity of ZnO in detail.[11–15] In the present experiment simple binary ZnO systems were used to investigate the effect of each dopant (including Li, Al, Mn, Co, and Cu) on the electrical conductivity of ZnO through the ac impedance spectroscopy.

Zinc oxide exhibits strong n-type conductivity with the electrons to move in the conduction band as charge carriers. In spite of extensive investigations, the source of such conductivity is still in debate. For many years the n-type conductivity has traditionally been attributed to native defects.[16,17] However, a recent first-principles investigation has revealed that, none of the native defects can provide a high-concentration shallow donor, but instead hydrogen is a promising candidate for the

* Corresponding author. Tel.: +81-52-789-4641; fax: +81-52-789-3233.
E-mail address: shushin@silky.numse.nagoya-u.ac.jp (Z. Zhou).

0955-2219/03/$ - see front matter © 2003 Elsevier Ltd. All rights reserved.
doi:10.1016/S0955-2219(03)00336-4

impurity causing the n-type conductivity in ZnO.[18] Experimental indications for hydrogen to behave as a donor in ZnO were reported in 1950s,[19] but no one paid attention to those results for many years. Recently, many researchers' interests have been focusing on hydrogen effects in ZnO.[20–28] In the present experiment hydrogen was also studied as a doping element, and hydrogen was introduced into ZnO by the ion implantation method.

2. Experimental procedure

2.1. Preparation of ZnO-based ceramic powder

The co-precipitation method was used for the preparation of the ZnO-based ceramic powders.[29] Such methods could improve the uniform distribution of the doping elements, as compared with the conventional method. Precipitation was conducted by adding the oxalic acid solution into the $Zn(CH_3COO)_2$ solution containing various doping ions, respectively. Here acetate salt (or nitrate salt) and oxalic acid were used as starting materials so as to avoid the introduction of disturbing ions such as Cl^- and Na^+. The precipitate was filtered, rinsed and dried. The calcination process of the precursor was analyzed using a thermo-gravimetric analyzer (MTS9000, ULVAC, Japan). Then the ZnO-based powders were obtained by calcining the precipitate at 500 °C for 2 h. The Li-doped ZnO powder was prepared by calcining the mixture of ZnC_2O_4 and $LiOH{\bullet}H_2O$ mixed in a conventional way[11] because of the high solubility of $Li_2C_2O_4$. The structure of the powder was analyzed with an X-ray diffractometer (XRD, RAD-IIC, Rigaku Co., Japan) using the Cu $K\alpha$ radiation, and the grain size of the powder was analyzed using a laser particle analyzer (LA-920, HORIBA, Japan). The contents of the dopants were analyzed by inductively coupled plasma (ICP) spectrometer (SPS 1500VR, SEIKO Instruments, Japan).

2.2. Sintering process of ZnO specimens

ZnO powders were consolidated into the disk-shaped specimens with 1.2 cm in diameter and 2–2.5 mm in thickness by the uniaxial pressing at 30 MPa in a mold, and then isostatically pressed at 150 MPa. Specimens were placed in crucibles and sintered in a muffle furnace, and the temperature of the furnace was controlled through programs. The sintering condition was kept as follows; specimens were kept at 1000 °C for 2 h, heated up to 1350 °C at the speed of 3 °C/min and then kept at this temperature for 3 h, and subsequently taken out of the furnace and cooled down to room temperature quickly in air. The sintered specimens were polished and observed using a scanning electron microscopy (SEM, S-3500H, Hitachi, Japan).

2.3. Electrical measurements

Sintered specimens were cut and polished into the shape of $0.8\times0.8\times0.03$ cm. After ultrasonic cleaning, the specimens were annealed at 1000 °C for 24 h to eliminate the surface mechanical damages caused during the polishing process, and after annealing the specimens were also cooled down to room temperature quickly in air. The In-Ga alloy was used to make ohmic electrodes for the electrical measurements. The dc electrical conductivity was measured with the HIOKI 3522-50 LCR HiTESTER. The ac impedance was measured with an impedance analyzer (3535 LCR HiTESTER and 3522-50 LCR HiTESTER, HIOKI, Japan). The modulus of complex impedance $|Z^*(\omega)|$ and phase angle $\theta(\omega)$ were recorded from the frequency 120 MHz to 1Hz at room temperature. The impedance spectra were simulated through the software ZView (Scribner Associates, Inc.). All the electrical measurements were conducted at room temperature.

2.4. Ion implantation of hydrogen into ZnO

The above ZnO thin specimen was doped with hydrogen using an ion implantation technique (ULVAC-PHI Inc., Japan). The H_2^+ ions were implanted into ZnO specimen using a 5 keV ion gun and the implantation dose was 1.44×10^{17} ions/cm^2. The contents of hydrogen in ZnO specimen were measured by the means of elastic recoil detection analysis (ERD, AN-2500, Nissin High Voltage Co., Ltd, Japan) before and after H_2^+ ions implantation. The ERD analysis was carried out using a He^+ beam of 1.7MeV energy. An aluminum filter was placed in front of the detector for the hydrogen detection.

3. Results and discussion

According to the X-ray diffraction analysis, all the ZnO samples had the Wurtzite structure, and no formation of other phase could be found for the doped ZnO specimens. The contents of the dopants are shown in Table 1. The content of Al was much lower than that in the starting solution due to the certain solubility of $Al_2(C_2O_4)_3$, but the effect of Al in ZnO was still observed apparently in the following measurements. All the sintered specimens had the apparent density over 5.4 g cm^{-3}, higher than 95% of the theoretical value, 5.67 g cm^{-3}. The color of the Li-doped ZnO and Al-doped ZnO is the same as that of the undoped ZnO, but the Mn-doped ZnO is orange, the Co-doped ZnO is green, and the Cu-doped ZnO is gray.

Table 1
The content of dopants in doped ZnO samples

Sample	Atomic ratio of dopant vs. zinc (ppm)
Li-doped ZnO	1152
Al-doped ZnO	363
Mn-doped ZnO	822
Co-doped ZnO	864
Cu-doped ZnO	1040

It is known that sintering and cooling conditions have great influences on the electrical conductivity of ZnO.[11, 30] In order to investigate the doping effects in the same condition, the experimental process was strictly controlled to keep identical as possible. Moreover, it was reported that slow cooling procedure enhanced the formation of resistive layer in the grain boundary, and caused the segregation of doping ions to the grain boundary,[12,31] so the fast cooling procedure was used in this investigation.

The dc electrical conductivity of the specimens was measured. Fig. 1 is the I–V curves for the undoped and doped ZnO specimens. In the measurement range all the specimens showed linear I–V characteristics, and the dc electrical conductivity could be calculated according to the curves.

3.1. Impedance spectra of ZnO specimens

Because the ac impedance spectroscopy can distinguish the conduction process in the grain and in the grain boundary, we used this method to investigate the effect of each dopant on the electrical conductivity in the grain and grain boundary of ZnO.

Fig. 2 shows the Cole–Cole plots for the impedance spectra of all the ZnO specimens. All the spectra contain only a single arc, but the arc has a non-zero intersection with the real axis in the high frequency region. The dc resistance (R_{dc}) can be estimated from the intersection between the arc and the real axis in the low frequency region. The dc resistance values were almost the same as those measured by the dc method in Fig. 1.

Jose et al.[32–34] and Nan et al.[35] have studied the impedance spectra for nanophase ZnO specimens. The impedance spectra of pure nanophase ZnO exhibited two arcs. The low frequency arc was interpreted as due to the grain boundary effect and the high frequency arc was attributable to the grain effect, in agreement with the conventional view. It should be noted that the above ZnO specimens were not sintered. In our experiment, the impedance spectra of the ZnO specimens without sintering were also measured. The specimens were prepared only by pressing and were coated with the conducting colloidal silver on both faces as electrodes, following the method of Jose et al.[32–34] There were also two arcs in the impedance spectrum, as shown in Fig. 3. Branković et al.[36] and Glot et al.[37] studied the impedance spectra of sintered and doped ZnO specimens, and only a single arc was observed in all the spectra. Even in the specimens without sintering, such as Al and Bi doped nanophase ZnO, there was only one arc in the

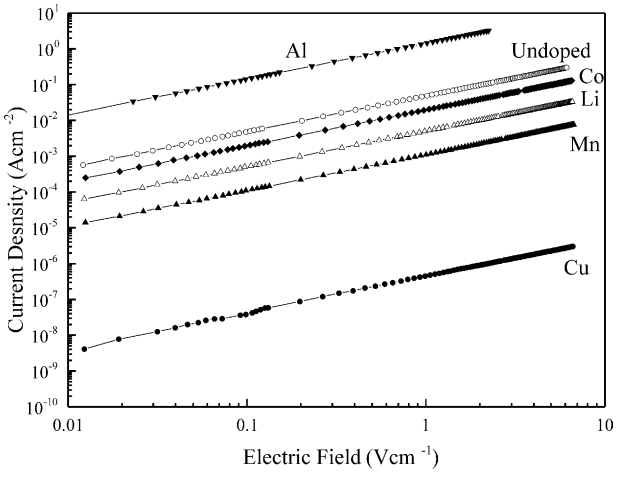

Fig. 1. I–V curves of undoped and doped ZnO specimens.

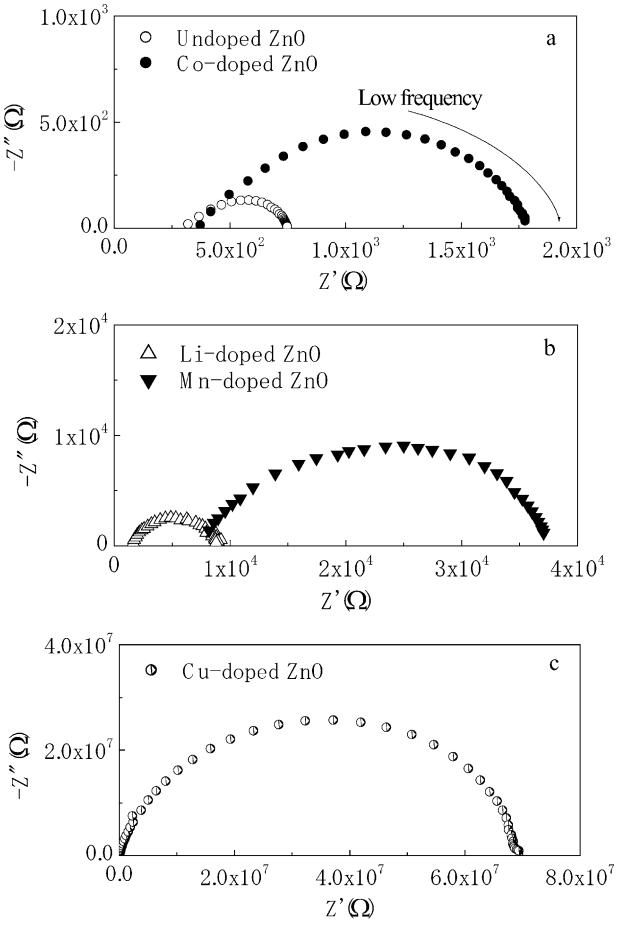

Fig. 2. Cole–Cole plots for the impedance spectra of undoped and doped ZnO specimens. (a) Undoped and Co-doped ZnO; (b) Li- and Mn-doped ZnO; (c) Cu-doped ZnO.

impedance spectra.[32–35] Some authors[33] thought that the one-arc spectrum means that the conduction processes through the grain and the grain boundary had identical time constants, τ. $\tau = 1/\omega = RC$, in which ω, R and C are peak frequency of the impedance arc, the resistance and the capacitance. That means that the conduction in the grain and the grain boundary occurs in the same process, so they can not be separated by the impedance spectroscopy. Other authors thought that the single arc was interpreted as due to the contribution from the grain boundary based on the model having resistive grain boundaries and conducting grain cores.[36]

In our experiment it was found that the arc in the impedance spectra of the sintered ZnO specimens became larger when the cooling rate decreased (in Fig. 4), in good agreement with the change trend of the grain boundary of ZnO.[11,30] So it is reasonable to attribute the arc to the response of the grain boundary region of ZnO. The ZnO specimens in Fig. 4 were sintered at 1300 °C for 5 h, but experienced different cooling process. The fast and slow cooling mean that the specimen was cooled down from 1300 to 900 °C within 0.5 and 2 h, respectively, and then taken out of the furnace to be cooled down to room temperature.

Based on the above analysis, the equivalent circuit shown in Fig. 5 was used to simulate all the experimental impedance spectra in this investigation. The resistance R_0 is attributed to the ZnO grains. R_1CPE_1 is attributed to the response of the grain boundary region of ZnO. In some ZnO varistor studies this part could further be divided into two parts because of the formation of the intergranular layer in the grain boundary region.[38,39] In the equivalent circuit, capacitance elements are represented by a constant phase element (CPE) with an admittance, $Y = Y_0(j\omega)^n$, where Y_0 is the admittance module, ω is the angular frequency and n is the frequency power factor of the CPE, which can indicate the level of the depression of the semicircle in the impedance spectrum. The experimental impedance data were well simulated using this equivalent circuit and the above parameters are shown in Table 2. The parameters R_0 and R_1 were used to estimate the grain and grain boundary electrical conductivity. The results are summarized in Fig. 6. The Al-doped ZnO specimens did not show an arc-shaped impedance spectrum, in agreement with the lack of the resistive grain boundary due to the Al doping. So only the total electrical conductivity is shown in Fig. 6 for the Al-doped ZnO.

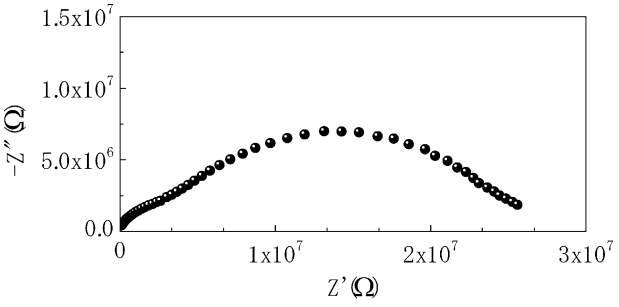

Fig. 3. The impedance spectrum of the ZnO specimen without sintering.

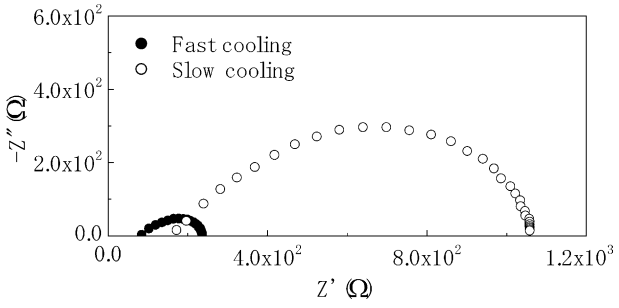

Fig. 4. The impedance spectra of ZnO specimens experienced different cooling process.

3.2. Effects of dopants on electrical conductivity of ZnO

It is evident from Fig. 6 that the Al-doped ZnO specimens had much higher electrical conductivity than the undoped ZnO, though the doping content was very low. It can be understood that the trivalent Al ions increase the electrical conductivity by forming a shallow donor in ZnO.[11,40,41] Also, the dc electrical conductivity of the Li-doped ZnO was lower than that of the undoped ZnO, and both the grain and grain boundary electrical conductivity were lower in the Li-doped ZnO than in the undoped ZnO, because the Li doping causes the formation of acceptor levels in ZnO.[42,43]

The Co doping had almost no obvious effects on the grain electrical conductivity of ZnO. There was a little effect on the grain boundary electrical conductivity. The doped Co ions in ZnO experienced the sintering process over 1000 °C, so they might be divalent, and they will not affect the electron concentration of ZnO. In other words, Co is considered to be a neutral impurity in ZnO.[44] It is well known that cobalt dopant is commonly

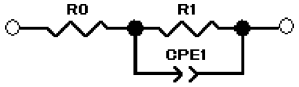

Fig. 5. Equivalent circuit for the simulation of the impedance spectra.

Table 2
Parameters separated from the spectra shown in Fig. 2

Sample	R_0 (Ω)	R_1 (Ω)	CPE_1 (F)	n
Undoped ZnO	3.22×10^2	4.25×10^2	9.64×10^{-10}	0.78
Co-doped ZnO	4.92×10^2	1.22×10^3	9.07×10^{-11}	0.89
Li-doped ZnO	1.61×10^3	7.22×10^3	1.09×10^{-10}	0.81
Mn-doped ZnO	6.97×10^3	3.15×10^4	1.65×10^{-9}	0.64
Cu-doped ZnO	2.43×10^5	6.80×10^7	2.91×10^{-11}	0.84

used in the ZnO varistor, since it leads to the formation of the potential barrier in the grain boundary. Many researchers have studied the effects of 3d transition metal impurities on the grain boundary of ZnO experimentally and theoretically. Most of them thought that 3d transition metal impurities could enhance the excess oxygen concentration in the grain boundary region,[44–46] and a potential barrier is formed there preferentially. However, in our results the Co doping effect was not so large, because of the very low doping content and the fast cooling process.

In contrast, the Mn doping had significant effects on the electrical conductivity of ZnO, though the doping content was very low. The electrical conductivity of the Mn-doped ZnO was apparently lower than that of the undoped ZnO, and the grain boundary was more resistive than the grain. It was regarded that Mn behaved as a deep donor in ZnO and depressed the concentration of intrinsic donors at the sintering temperature. When the specimens were cooled to room temperature quickly, the condition at the sintering temperature could be frozen and the concentration of the intrinsic donors would also be low at room temperature.[11–15] Due to the same effects of all the 3d transition metal on the adsorbed oxygen in the grain boundary region, the effect of Mn doping was greater on the grain boundary than on the grain, so the grain boundary was more resistive than the grain. Mn is also a commonly used dopant in the ZnO varistor to build up the potential barrier in the grain boundary.

The Cu-doped ZnO specimen was the most resistive, and the electrical conductivity was 5 orders of magnitude lower than that of the undoped ZnO. Both the grain and grain boundary electrical conductivity decreased significantly by the Cu doping. When the Cu-doped ZnO was experienced high temperature over 1000 °C, Cu could exist in ZnO as Cu^+, which is probably more stable at high temperatures. The reports of Fons et al.[47] proved that the valence of Cu was +1 in the Cu-doped ZnO. The Cu^+ ions are substituted for Zn^{2+} ions in the ZnO lattice and behave as an acceptor-type impurity.[48–50] Since the extrinsic donor is absent in the Cu-doped ZnO specimen, Cu^+ has to be compensated by either the intrinsic donor or the hole to keep the electroneutrality, the electrical conductivity in the n-type ZnO semiconductor decreased greatly by the Cu doping. The acceptors will be compensated by electrons in the grain because there are some intrinsic donors there. However, since the concentration of the intrinsic donors is much lower in the grain boundary, the acceptors have to be compensated by the holes in this region. Moreover, the Cu doping also had a great effect on the grain boundary because of the same interaction with ambient oxygen as the other 3d transition metal impurities. Due to the above two reasons, the grain boundary of the Cu-doped ZnO specimens was more resistive than the grain. The grain boundary was over 2 orders of magnitude more resistive than the grain, and the total resistance of the Cu-doped ZnO specimens was almost completely caused by the grain boundary. In common ZnO varistors, the grain boundary is several orders of magnitude more resistive than the grain, so it is natural to attribute the impedance spectra completely to the response of the grain boundary, and the contribution of the grain could be neglected. Though the doping content of Cu was very low and the specimens were experienced fast cooling process in our experiment, the Cu-doped ZnO specimens should have some varistor properties according to the results in Table 2. However, the Cu-doped ZnO did not show the nonlinear I–V curve in Fig. 1, since the electric field strength in our measurement was too low to reach the leakage voltage of this varistor. In Kutty and Raghu's report[49] the measurement range was about 1–1000 V/cm. Cu can be an effective doping element to build up the potential barrier in the grain boundary of ZnO.

The doping of various metal ions might have effects on the defect chemistry of ZnO, which will not be discussed in the present paper, and deeper investigation is necessary.

3.3. Hydrogen effect on the electrical conductivity of ZnO

In this experiment, the sintered bulk ZnO specimens were used for the study of the hydrogen effect on the electrical conductivity of ZnO. The sintered specimen was thinned down to about 0.3 mm, and then, the H_2^+ implantation was applied to the specimen surface. The thickness of the implanted layer on the surface was about 200 nm, much thinner than the total specimen thickness, 0.3 mm. So, for the electrical conductivity measurement a parallel circuit was made between the implanted layer and the rest of the specimen (i.e. the substrate).

Fig. 7 is the result of the ERD analysis for the ZnO specimen before and after H_2^+ implantation. It was seen from this figure that, hydrogen ions really existed in the common ZnO specimen, even before the hydrogen ion implantation. This result can prove that hydrogen is a very plausible impurity unintentionally incorporated into ZnO in the preparation process. After hydrogen ion implantation, the count of hydrogen ions increased greatly. As a result, the electrical conductivity of the specimen also increased apparently, as shown in Fig. 8. In the impedance spectrum the arc disappeared after hydrogen ion implantation and showed the same impedance behavior as the Al-doped ZnO. This might indicate the elimination of the resistive grain boundary by the introduction of hydrogen into this region. Kohiki et al[51] and Arita et al[25] studied the effects of hydrogen introduced into ZnO thin film through ion implantation

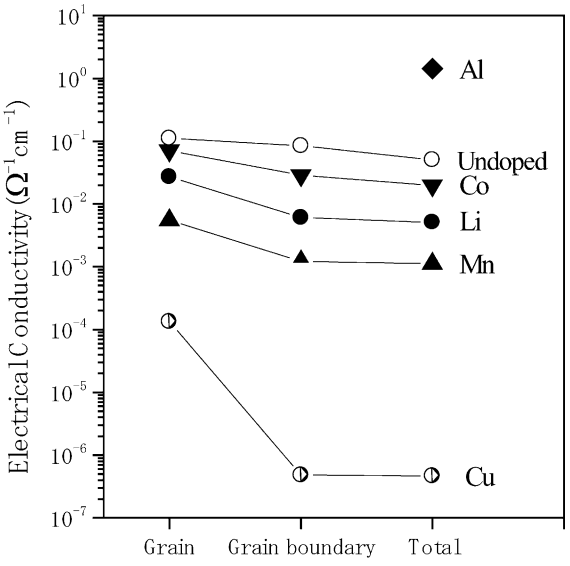

Fig. 6. Changes of the grain, grain boundary and total electrical conductivity with dopants.

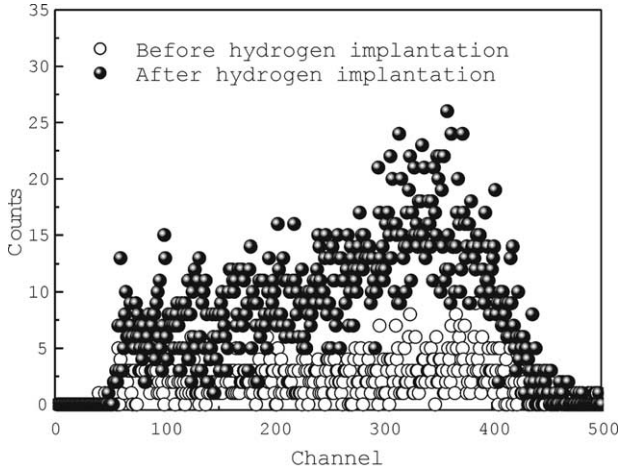

Fig. 7. ERD analysis for the ZnO specimen before and after hydrogen implantation.

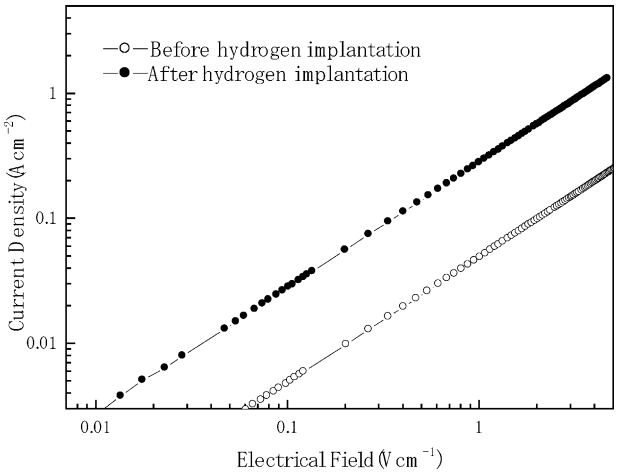

Fig. 8. I–V curves for undoped ZnO specimen before and after hydrogen implantation.

method. Kohiki et al.[51] reported that the electrical conductivity of ZnO thin film rose from 1×10^{-7} to 5.5×10^{2} Ω^{-1}cm^{-1}. Also, Arita et al.[25] obtained over five orders of magnitude increase of the electrical conductivity in their experiment. It should be noted that the above results were obtained in ZnO thin film, with the thickness of 2000 and 150 nm, respectively. Moreover, the ZnO film used in the experiment by Kohiki et al.[51] was very resistive. If the surface layer, in which H_2^+ was implanted, is considered to be about 200nm in thickness, and the other part of the ZnO specimen is regarded as a substrate, then the electrical conductivity of the implanted layer alone could increase from 5×10^{-2} to 3.5×10^{2} Ω^{-1}cm^{-1}, approaching to the results of Arita et al.[25] In our other experiment, when hydrogen ions were implanted into the highly resistive Cu-doped ZnO specimens, the electrical conductivity in the hydrogen-implanted layer also increased about 9 orders of magnitude, which will be reported elsewhere.[52]

It has been theoretically predicted that hydrogen forms a shallow donor level in ZnO,[28] so the electrical conductivity increased greatly. This is the effect of hydrogen that has recently been regarded as the source of the n-type conductivity of ZnO. It is in contrast to the traditional idea that native defects cause the n-type conductivity. The recent first-principles calculation revealed that none of the native defects exhibits characteristics consistent with a high-concentration shallow donor. Hydrogen is an excellent candidate for the impurity that is unintentionally incorporated into ZnO.[18] The H^+ ions in ZnO can move readily from the interstitial site to the neighboring oxygen site and forms OH ions in the form of $(O_oH_i)^{\bullet}$. Here O_o, H_i and $^{\bullet}$ represent the O atom on the oxygen lattice site, H atom in the interstitial site, and the singly ionized donor, respectively. According to the calculation results, the $(O_oH_i)^{\bullet}$ unit can be regarded as a new type of donor delivering an electron into the conduction band, which can turn the oxygen into a sort of doping element, in agreement with the present experimental results.

4. Conclusions

The effects of various dopants on the electrical conductivity of ZnO were studied in simple binary systems using the ac impedance spectroscopy. The Al doping increased the dc electrical conductivity by about two orders of magnitude. The electrical conductivity of the Li-doped ZnO was lower than that of the undoped ZnO. Moreover, both the grain and grain boundary electrical conductivity were lower in the Li-doped ZnO than in the undoped ZnO, because the Li doping led to the formation of acceptor levels. The doping of all the

3d transition metal impurities (Mn, Co, and Cu) had effects on the grain boundary and made the grain boundary region more resistive. The grain boundary of Cu-doped ZnO was the most resistive one. The Co doping had almost no effects on the grain electrical conductivity, Mn made the grain a little more resistive, and the Cu doping yielded the grain electrical conductivity by two orders of magnitude lower than that of the undoped ZnO.

Hydrogen was also investigated as a doping element in ZnO, and hydrogen was introduced into ZnO by the ion implantation method. The electrical conductivity in the hydrogen-implanted layer increased from 5×10^{-2} to 350 $\Omega^{-1}cm^{-1}$.

Acknowledgements

The authors would like to thank Dr. Jiaping Han for the helpful advice on the electrical measurements of ZnO specimens. One of the authors (Zhen Zhou) also thanks the financial support from the Japan Society for the Promotion of Science (JSPS). This study was supported by a Grant-in-Aid for Scientific Research from the Ministry of Education, Culture, Sports, Science and Technology of Japan.

References

1. Look, D. C., Recent advances in ZnO materials and devices. *Mater. Sci. Eng.*, 2001, **B80**, 383–387.
2. Gupta, T., K, Application of zinc oxide varistors. *J. Am. Ceram. Soc.*, 1990, **77**(7), 1817–1840.
3. Costa, M. E. V., Mantas, P. Q. and Baptista, J. L., Effect of electrode alterations on the ac behaviour of Li_2O-ZnO humidity sensors. *Sens. Actuator, B26–27*, 1995, 312–314.
4. Scarano, D., Bertarione, S., Spoto, G., Zecchina, A. and Otero Arean, C., FTIR spectroscopy of hydrogen, carbon monoxide, and methane adsorbed and co-adsorbed on zinc oxide. *Thin Solid Films*, 2001, **400**, 50–55.
5. Ismail, B., Abaab, M. and Rezig, B., Structural and electrical properties of ZnO films prepared by screen printing technique. *Thin Solid Films*, 2001, **383**, 92–94.
6. Clark, D. R., Varistor ceramics. *J. Am. Ceram. Soc.*, 1999, **82**(3), 485–502.
7. Gambino, J. P., Kingery, W. D., Pike, G. E., Philipp, H. R. and Levinson, L. M., Grain boundary electronic states in some simple ZnO varistors. *J. Appl. Phys.*, 1987, **61**(7), 2571–2574.
8. Mukae, K., Tsuda, K. and Nagasawa, I., Non-ohmic properties of ZnO-rare earth metal oxide-Co_3O_4 ceramics. *Jpn. J. Appl. Phys.*, 1977, **16**(8), 1361–1368.
9. Matsuoka, M., Nonohmic properties of zinc oxide ceramics. *Jpn. J. Appl. Phys.*, 1971, **10**(6), 736–746.
10. Hoon, H. H. and Ling, C. P., Effects of MnO_2 doping in V_2O_5-doped ZnO varistor system. *Mater. Chem. Phys.*, 2002, **9347**, 1–6.
11. Han, J., Mantas, P. Q. and Senos, A. M. R., Effect of Al and Mn doping on the electrical conductivity of ZnO. *J. Eur. Ceram. Soc.*, 2001, **21**, 1883–1886.
12. Han, J., Senos, A. M. R. and Mantas, P. Q., Varistor behaviour of Mn-doped ZnO ceramics. *J. Eur. Ceram. Soc.*, 2002, **22**, 1653–1660.
13. Han, J., Senos, A. M. R. and Mantas, P. Q., Nonisothermal sintering of Mn doped ZnO. *J. Eur. Ceram. Soc.*, 1999, **19**, 1003–1006.
14. Han, J., Senos, A. M. R. and Mantas, P. Q., Deep donors in polycrystalline Mn-doped ZnO. *Mater. Chem. Phys.*, 2002, **75**, 117–120.
15. Han, J., Mantas, P. Q. and Senos, A. M. R., Defect chemistry and electrical characteristics of undoped and Mn-doped ZnO. *J. Eur. Ceram. Soc.*, 2002, **22**, 49–59.
16. Look, D. C., Hemsky, J. W. and Sizelove, J. R., Residual native shallow donor in ZnO. *Phys. Rev. Lett.*, 1999, **82**, 2552–2555.
17. Sun, Y., Xu, P., Shi, C., Xu, F., Pan, H. and Lu, E., A FT-LMTO study on the native shallow donor in ZnO. *J. Electron. Spectrosc. Relat. Phenom., 114–116*, 2001, 1123–1125.
18. Van de Walle, C. G., Hydrogen as a cause of doping in zinc oxide. *Phys. Rev. Lett.*, 2000, **85**, 1012–1015.
19. Tomas, D. G. and Lander, J. J., Hydrogen as a donor in zinc oxide. *J. Chem. Phys.*, 1956, **25**, 1136–1142.
20. Hofmann, D. M, Hofstaetter, A., Leiter, F., Zhou, H., Henecker, F., Meyer, B. K., Orlinskii, S. B., Schmidt, J. and Baranov, P. G., Hydrogen: a relevant shallow donor in zinc oxide. *Phys. Rev. Lett.*, 2002, **88** (045504-1-045504-4).
21. Shimomura, K., Nishiyama, K. and Kadono, R., Electronic structure of the muonium center as a shallow donor in ZnO. *Phys. Rev. Lett.*, 2002, **89** (255505-1-4).
22. Han, C. S., Jun, J. and Kim, H., The depth of depletion layer and the height of energy barrier on ZnO under hydrogen. *Appl. Surf. Sci.*, 2001, **175-176**, 567–573.
23. Ohashi, N., Ishigaki, T., Okada, N., Sekiguchi, T., Sakaguchi, I. and Haneda, H., Effect of hydrogen doping on ultraviolet emmision spectra of various types of ZnO. *Appl. Phys. Lett.*, 2002, **80**, 2869–2871.
24. Cox, S. F., Davis, E. A., Cottrell, S. P., King, P. J., Lord, J. S., Gil, J. M., Alberto, H. V., Vilão, R. C., Piroto Duarte, J., Ayres de Campos, N., Weidinger, A., Lichti, R. L. and Irvine, S. J., Experimental confirmation of the predicted shallow donor hydrogen state in zinc oxide. *Phys. Rev. Lett.*, 2001, **86**, 2601–2604.
25. Arita, M., Konishi, H., Matsuda, K., Masuda, M. and Hayashi, Y., Effects of Hydrogen Introduction on Electrical and Optical Properties of Cd-doped Ge Oxide and Zn Oxide Thin Films. *Mater. Trans.*, 2002, **43**(5), 1142–1145.
26. Kang, Y.-S., Kim, H.-Y. and Lee, J.-Y., Effects of hydrogen on the structural and electro-optical properties of zinc oxide thin film. *J. Electrochem. Soc.*, 2000, **147**(12), 4625–4629.
27. Baik, S. J., Jang, J. H., Lee, C. H., Cho, W. Y. and Lim, K. S., Highly textured and conductive undoped ZnO film using hydrogen post-treatment. *Appl. Phys. Lett.*, 1997, **70**, 3516–3518.
28. Van de Walle, C. G., Defect analysis and engineering in ZnO. *Phys. B*, 2001, **308–310**, 899–903.
29. Takehana, M., Nishino, T., Sugawara, K. and Sugawara, T., Preparation of zinc varistor by a wet chemical method. *Mater. Sci. Eng.*, 1996, **B41**, 186–189.
30. Wong, J., Microstructure and phase transformation in a highly non-ohmic metal oxide varistor ceramic. *J. Appl. Phys.*, 1975, **46**(4), 1653–1659.
31. Raghu, N. and Kutty, T. R. N., Relationship between nonlinear resistivity and the varistor forming mechanism in ZnO ceramics. *Appl. Phys. Lett.*, 1992, **60**(1), 100–102.
32. Jose, J. and Abdul Khadar, M., Role of grain boundaries on the electrical conductivity of nanophase zinc oxide. *Mater. Sci. Eng.*, 2001, **A304-306**, 810–813.
33. Jose, J. and Abdul Khadar, M., Impedance spectroscopic analysis of ac response of nanophase ZnO and ZnO-Al_2O_3 nanocomposites. *Nanostruct. Mater.*, 1999, **11**(8), 1091–1099.
34. Jose, J. and Abdul Khadar, M., Role of grain boundaries on the electrical properties of ZnO-Ag nanocomposites: an impedance spectroscopic study. *Acta Mater.*, 2001, **49**, 729–735.

35. Nan, C. W., Tschöpe, A., Holten, S., Kliem, H. and Birringer, R., Grain size-dependent electrical properties of nanocrystalline ZnO. *J. Appl. Phys*., 1999, **85**(11), 7735–7740.
36. Brankoviæ, Z., Brankoviæ, G., Poleti, D. and Varela, J. A., Structural and electrical properties of ZnO varistors containing different spinel phases. *Ceram. Int*., 2001, **27**(1), 115–122.
37. Glot, A., Di Bartolomeo, E. and Traversa, E., Humidity sensitive electrical properties of a novel ceramic Heterocontact structure $ZnO/BaPb_{0.8}Bi_{0.2}O_3$. *J. Eur. Ceram. Soc*., 1999, **19**, 715–719.
38. Matsuura, M. and Yamaoki, H., Dielectric dispersion and equivalent circuit in nonohmic ZnO ceramics. *Jpn. J. Appl. Phys*., 1977, **16**(7), 1261–1262.
39. Andres-Verges, M. and West, A. R., Impedance and modulus spectroscopy of ZnO varistors. *J. Electroceramics*, 1997, **1**, 2 125-132.
40. Tsal, Y. L., Huang, C. L. and Wei, C. C., Improvement of nonlinearity in a ZnO varistor by Al_2O_3 doping. *J. Mater. Sci. Lett*., 1985, **4**, 1305–1307.
41. Jäger, S. and Szyszka, B., Optical and electrical properties of doped zinc oxide films prepared by ac reactive magnetron sputtering. *J. Non-Crystalline Solids*, 1997, **218**, 74–80.
42. Fijihara, S., Sasaki, C. and Kimura, T., Effects of Li and Mg doping on microstructure and properties of sol-gel ZnO thin films. *J. Eur. Ceram. Soc*., 2001, **21**, 2109–2112.
43. Inoue, M., A model for the acceptor state in II–VI compounds. *J. Phys. Chem. Solids*, 1979, **40**, 857–862.
44. Ohashi, N., Terada, Y., Ohgaki, T., Tanaka, S., Tsurumi, T., Fukunaga, O., Haneda, H. and Tanaka, J., Synthesis of ZnO bicrystals doped with Co or Mn and their electrical properties. *Jpn. J. Appl. Phys*., 1999, **38**, 5028–5032.
45. Oba, F., Tanaka, I. and Adachi, H., Effect of oxidation on chemical bonding around 3d transition-metal impurities in ZnO. *Jpn. J. Appl. Phys*., 1999, **38**, 3569–3575.
46. Mantas, P. Q. and Baptista, J. L., The barrier height formation in ZnO varistors. *J. Eur. Ceram. Soc*., 1995, **15**, 605–615.
47. Fons, P., Nakahara, K., Yamada, A., Iwata, K., Matsubara, K., Takasu, H. and Niki, S., A XANES study of Cu valency in Cu-doped epitaxial ZnO. *Phys. Stat. Sol*., 2002, **229**(2), 849–852.
48. Bellini, J. V., Morelli, M. R. and Kiminami, R. H. G. A., Electrical properties of polycrystalline ZnO:Cu obtained from freeze-dried ZnO + copper(II) acetate powders. *J. Mater. Sci.—Mater. Electron*., 2002, **13**, 485–489.
49. Kutty, T. R. N. and Raghu, N., Varistors based on polycrystalline ZnO:Cu. *Appl. Phys. Lett*., 1989, **54**(18), 1796–1798.
50. Jun, S.-T. and Choi, G. M., Composition dependence of the electrical conductivity of ZnO(n)–CuO(p) ceramic composite. *J. Am. Ceram. Soc*., 1998, **81**(3), 695–699.
51. Kohiki, S., Nishitani, M., Wada, T. and Hirao, T., Enhanced conductivity of zinc oxide thin films by ion implantation of hydrogen atom. *Appl. Phys. Lett*., 1994, **64**(21), 2876–2878.
52. Zhou, Z., Kato, K., Komaki, T., Yoshino, M., Yukawa, H., Morinaga, M. and Morita, K., Electrical conductivity of Cu-doped ZnO and its change with hydrogen implantation. *J. Electroceram*. (submitted for publication).